International Journal of Modern Physics C
Vol. 18, No. 2 (2007) 163–175

World Scientific
www.worldscientific.com

ON DIRECTLY SOLVING SCHRÖDINGER EQUATION FOR H_2^+ ION BY GENETIC ALGORITHM

RAJENDRA SAHA* and S. P. BHATTACHARYYA†

Department of Physical Chemistry
Indian Association for the Cultivation of Science
Jadavpur, Calcutta-700032, India
†*pcspb@mahendra.iacs.res.in*

Received 24 December 2005
Revised 17 February 2006
Accepted 11 March 2006

Schrödinger equation (SE) is sought to be solved directly for the ground state of H_2^+ ion by invoking genetic algorithm (GA). In one approach the internuclear distance (R) is kept fixed, the corresponding electronic SE for H_2^+ is solved by GA at each R and the full potential energy curve (PEC) is constructed. The minimum of the PEC is then located giving V_e and R_e. Alternatively, V_e and R_e are located in a single run by allowing R to vary simultaneously while solving the electronic SE by genetic algorithm. The performance patterns of the two strategies are compared.

Keywords: Soft-computing and Schrödinger equation; genetic algorithm; artificial intelligence driven solution of Schrödinger equation.

1. Introduction

H_2^+ is the simplest three particle (2 nuclei and 1 electron) molecular system with a stable bound state. The equilibrium geometry and well depth are well-characterized both theoretically and experimentally. If the nuclear positions are held fixed, as is customary under the Born–Oppenheimer (BO) approximation, the electronic SE separable and can be solved with any degree of accuracy[1] for each internuclear separation. The ground state potential energy curve [$V(R)$] is characterized by a well defined minimum (V_e, R_e) and asymptotically and smoothly leads to the dissociation limit H(1S) + H^+ as $R \to \infty$. Many variational calculations, too are available in the literature[2–5] with varying degrees of accuracy. Different types of basis sets have been used here in variational calculation. A finite element method with a very large basis of a new type has been reported.[6] Potential energy curves

*Present address: Haldia Govt. College, P. O. Debhog, West Bengal 721 657, India.
†Corresponding author.

including nonadiabatic corrections for the ground and excited states of H_2^+ too, are available.[7–9] The system can therefore serve as a benchmark for new techniques of solving molecular electronic SE. We note that almost all the currently available methodologies of solving problems of molecular electronic structure are dominantly variational and basis set dependent. The techniques used are also generally deterministic. However, reports on successful diffusion Monte Carlo calculations on H_2^+ and H_2 are available[10] in the literature.

Recently, genetic algorithm has been invoked by different groups for solving SE for bound states of atomic and model Hamiltonians.[11–18] These applications are still at a rudimentary level; nevertheless, they indicate interesting possibilities of further developments. To the best of our knowledge the *workability of a GA-based systematism for solving the molecular electronic SE directly has not been demonstrated yet*. On the other hand, such a demonstration would undoubtedly generate more interest in exploring GA in the context of solving molecular electronic SE. The purpose of the present communication has been primarily to explore if the GA-based strategy proposed[11–18] for handling the SE for one and two electron atoms remains viable in the molecular context (e.g., H_2^+) as well. Although the present problem can be reduced to an effectively one dimensional problem, we would prefer to treat it as a three-dimensional problem in Cartesian coordinates primarily to assess the possibility of using the GA-based technique for handling problems of higher dimensions. Two different strategies are developed. In the first, the electronic SE of the ground state of H_2^+ is solved as a 3D problem for a set of fixed nuclear frameworks (that is, for different values of internuclear separation R) and the results are combined to produce the potential energy curve of H_2^+ and locate the equilibrium internuclear separation R_e. In the second, the molecular SE is solved by GA without keeping the internuclear separation fixed. GA is allowed to search out simultaneously the equilibrium internuclear separation (R_e) and optimal electronic probability amplitude distribution in the three dimensional space of electronic coordinates consistent with R_e. The evolving probability amplitude distribution is described in a three-dimensional discretized Cartesian coordinate space. A natural question is then how the choice of grid affect the final results. We have looked into the possible magnitudes of discretization error. The behavior of the GA-based wavefunction as the inter nuclear separation (R) reaches the dissociation limit ($R \to \infty$) has also been investigated with particular emphasis on the choice of initial population so that the wave function correctly reproduces the expected behavior in the dissociation limit. The layout of the paper is as follows. In Sec. 2, we describe the system and methodology to be used while in Sec. 3 the results are presented.

2. Method

The coordinate system used to represent the hydrogen molecule ion (H_2^+) is depicted in the figure below. The internuclear axis is taken to be the z-axis with the origin being at the midpoint O of the internuclear axis.

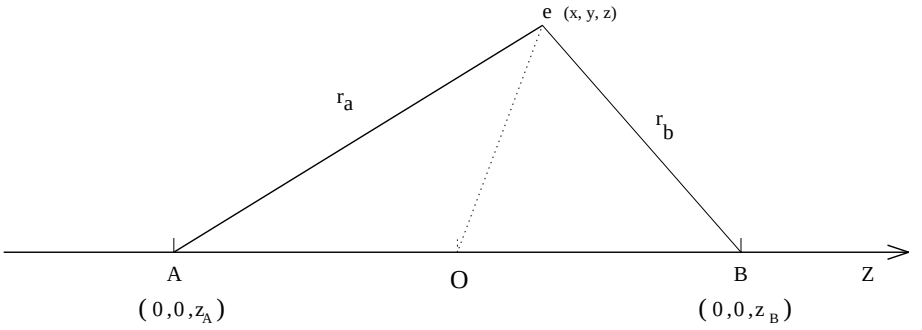

The internuclear separation between the two hydrogen nucleii is R ($z_A = -R/2, z_B = R/2$), O, the midpoint of A–B being the origin. In the fixed nucleus approximation, the Hamiltonian describing the motion of the electron is represented as

$$H = -\frac{\hbar^2}{2m}\left(\frac{\partial^2}{\partial x^2} + \frac{\partial^2}{\partial y^2} + \frac{\partial^2}{\partial z^2}\right) - \left(\frac{e^2}{r_A} + \frac{e^2}{r_B}\right) + \frac{e^2}{R} \tag{1}$$

where $r_A = \sqrt{(x^2 + y^2 + (z - z_A)^2)}$, $r_B = \sqrt{(x^2 + y^2 + (z - z_B)^2)}$, the electron being assigned the coordinates x, y, z. The energy eigenstates of H_2^+ are described by the eigenvalue equation

$$H(R)\psi_n(R) = E_n(R)\psi_n(R)\,. \tag{2}$$

Our interest in this communication concerns the ground state which at a fixed internuclear separation is presented as an appropriate probability amplitude distribution $\{\phi(x_i, y_i, z_i)\}$ in the discretized three-dimensional space. In Type I of the GA-based approach we start with a population of discretized probability amplitude distributions $\{\Phi_I(x_i, y_j, z_k)\}_{I=1,2,\ldots,n_p}$, n_p being the population size. The indices i, j, k run from $(1, n_x)$, $(1, n_y)$, $(1, n_z)$, respectively. The set of $n_x \times n_y \times n_z$ numbers for each I are collected in one-dimensional arrays S_I are called wave-function strings and each string is characterized by a fitness value f_I which is defined in three steps as follows. The energy E_I corresponding to the string S_I is first defined:

$$E_I = \frac{\langle S_I|H|S_I\rangle_s}{\langle S_I|S_I\rangle_s} \tag{3}$$

where $\langle\rangle_s$ refers to analytical integration being replaced by summation (quadrature). An objective function $\mathcal{F}_I$ is then constructed by taking

$$\mathcal{F}_I = (E_I - E_L)^2 \tag{4}$$

E_L being the estimated lower bound to the ground state energy of H_2^+. The fitness of the Ith string is finally defined by setting,

$$f_I = e^{-\lambda \mathcal{F}_I} \tag{5}$$

λ being a "user chosen" scalar that prevents exponential overflow/underflow. The kinetic energy component of E_I is computed by three-dimensional Fast Fourier

Transform (FFT).[19] The potential energy is computed by direct quadrature using Trapezoid or Simpson's rule. The starting wavefunction strings were generated from different sets of functions (symmetrized as well as asymmetric) like

$$\begin{aligned}
\psi(x,y,z) \equiv\ & N_1(e^{-(\alpha r_a+\beta r_b)} + e^{-(\beta r_a+\alpha r_b)}) && \text{(symmetrized)} \\
& N_2 e^{-(\alpha r_a+\beta r_b)} && \text{(nonsymmetric)} \\
& N_3(1+\gamma r_A)[e^{-(\alpha' r_A+\beta' r_B)}] && \text{〃} \\
& N_4(1+\gamma' r_B)[e^{-(\alpha'' r_A+\beta'' r_B)}] && \text{〃} \qquad (6)
\end{aligned}$$

where α, β, α', β', γ', α'', β'', γ'' etc. are chosen randomly, in the range $0 < \alpha$, $\beta, \ldots, < 1$.

The initial or the trial population of wavefunction strings are allowed to evolve under the action of the set of operators, like selection, crossover and mutation.[10] We have chosen 20% of the strings at any stage of the evolution by the standard Roulette wheel procedure (fitness proportional selection) while the remaining strings were randomly chosen from the current population.

Simple one point arithmatic crossover[12] with probability p_c was applied to the randomly chosen pairs of strings. Let S_k and S_l be the two one-dimensional arrays representing the probability amplitude distributions in the ground state of H_2^+ ion at a given internuclear separation.

$$S_k = (a_1, a_2 \cdots a_k \cdots a_n) \qquad (7)$$

$$S_l = (b_1, b_2 \cdots b_k \cdots b_n)\,. \qquad (8)$$

If the kth site is chosen for crossover with a probability p_c, the two post crossover strings S'_k and S'_l are defined as follows

$$S'_k = (a_1, a_2, \ldots, a_k, a'_{(k+1)} \cdots a'_n) \qquad (9)$$

$$S'_l = (b_1, b_2, \ldots, b_k, b'_{(k+1)} \cdots b'_n) \qquad (10)$$

where

$$a'_l = f a_l + (1-f) b_l \qquad (11)$$

$$b'_l = (1-f) a_l + f b_l \qquad (12)$$

with f randomly chosen in (0, 1). For the optimization of the probability amplitude distribution coded by the strings at shorter internuclear distances (lying around equilibrium region of the potential energy curve) the crossover operation was designed in such a way that points lying in the internuclear region or closer to the nucleii were sampled more frequently[13] than those lying far away, while for longer internuclear distances (lying around the dissociation limit of the potential energy curve) the positions away from the internuclear region were sampled relatively more frequently. Arithmatic mutation operation was carried out with a probability p_m

as follows. If the kth site of the string S'_k is chosen for mutation with a probability p_m, the mutated amplitude is computed by taking

$$a'_k = a_k + r(-1)^l \Delta \tag{13}$$

where r is a random number in (0, 1), Δ is the mutation intensity and l is a randomly chosen integer. Following the crossover and mutation operations, the newly generated wavefunction strings were symmtrized as follows:

(a) The left-right symmetrization along the internuclear axis (z-axis) was carried out by setting

$$\Phi(x_i, y_j, -z_k) = \Phi(x_i, y_j, z_k)\,. \tag{14}$$

The forcible symmetrization was avoided for calculations at longer internuclear distances to allow the electronic amplitude distribution the freedom to get distorted as $R \to \infty$ and H_2^+ dissociates into H(1s) + H^+.

(b) The other type of symmetry enforced on the amplitude distribution concerns equivalance of the other two axes (x, y) and this was ensured by demanding

$$\Phi(x_i, y_j, z_k) = \Phi(y_j, x_i, z_k)\,. \tag{15}$$

The set of genetic operations described so far ultimately drives the population to the optimum amplitude distribution at the internuclear separation R and consequently to the optimal energy for the particular nuclear configuration $V(R)$. Results of the calculation for many such values of R are combined to generate the potential energy curve $V(R)$, the minimum of which is the ground state energy and the correspondig $R = R_e$ is the equilibrium internuclear separation (R_e). We have designated this approach as Type I.

In the Type II version of GA-based search the ground state of H_2^+, The wavefunction strings have the internuclear separation R_l encoded into them so that S_Is now read

$$S_I(i, j, k, l) \equiv \Phi_I(x_i, y_j, z_k, R_l)\,, \tag{16}$$

$i = 1, 2, \ldots, n_x; \cdots j = 1, 2, \ldots, n_j; \cdots k = 1, 2, \ldots, n_k; \cdots l = 1, 2, \ldots, n_l$, meaning that Φ_I is the probability amplitude for the electron at a point in space $P \equiv x_i$, y_j, z_k when the internuclear distance between the two hydrogen nucleii is R_l. Now, crossover and mutation operations would change not only the amplitude but also the internuclear distance and the genetic evolution could lead to the global energy minimum V_e and internuclear distance R_e corresponding to V_e, in a single run. This strategy leads to a coupled evolution of the electron probability amplitudes and the internuclear separation towards the global minimum.

3. Results and Discussion

We present the results of our calculations in two sets (Set I and Set II) each under Type I and Type II. Type I presents results of calculations of the ground state

wave function and energy of H_2^+ at several values of internuclear separation $E(R)$, construction of the PEC, and extraction of R_e and V_e values. In Type II calculations, R is allowed to be optimized simultaneously with the ground state electronic probability amplitude distribution, so that R_e, V_e values are determined along with the optimal amplitude distribution in a single run. The Set I refers to calculations with a smaller number of grid points while Set II results correspond to calculations with a larger number of grid points.

3.1. *Results of Type I calculation*

Set I: We report results of calculations carried out with a coordinate grid of 64 points along each axis: $n_x = 64$, $n_y = 64$, $n_z = 64$ so that the amplitude distribution is described over a total number of $64 \times 64 \times 64$ points in the space concerned. A population size $n_p = 10$ has been uniformly used. Crossover probability has been held fixed at $p_c = 0.75$ and information mixing parameter f in the arithmetic crossover was designed to vary in the range $0.5 \leftrightarrow 1$. The functional form chosen for the variation of f is $f = f_c \pm 0.5 \times \alpha_c$ where α_c is a random number in the range $0 \leftrightarrow 1$ and $f_c = 0.5$. The mutation probability has been held fixed at $p_m = 0.05$ and the mutation intensity Δ is assumed to be a continuously changing function of the number of generations (n_g). The specific form chosen in the present calculation is[13]

$$\Delta(n_g, y) = y[1 - r^{(1-n_g/T)^l}] \tag{17}$$

where r is a random number in the range $0 \leq r \leq 1$, T is the maximum number of generations during which the evolution would take place, l is a system dependent parameter ($l = 2$ has been used) while y is chosen from a specified range ($b_{\min} \leq y \leq b_{\max}$). When the parameters are chosen in this manner, $\Delta \to 0$ as $n_g \to T$.

Figure 1(a) shows the computed probability density plot at $R = 2.0$ a.u. with the symmetrization condition of Eq. (15) enforced. The plot reveals perfect inversion symmetry about the origin as it should. The computed energy at $R = 2.0$ a.u. turns out to be -0.58712 a.u. It may be noted that at such short internuclear distances the symmetry of the probability distribution is preserved even if the symmetrization condition of Eq. (14) is not enforced. The evolution of the energy computed with the best string during the run is presented in Fig. 1(b). The energy improves in steps and then saturates out. Figures 2(a)–2(c) display the plots of computed probability densities at $R = 4.0$, 5.6 and 7.2 a.u., respectively, without the symmetrization condition of Eq. (14) being enforced. One can easily notice the distortion of the probability density as R increases, revealing that the dissociation behavior of H_2^+ into H(1s) + H^+ is being correctly simulated by GA as $R \to \infty$.

The minimum values of energy computed at different values of the internuclear distance R are shown in Fig. 3. The profile has been fitted to a Morse-curve and the predicted equilibrium values of R_e and D_e are reported in Table 1. The asymptotic dissociation behavior is correctly reproduced in Fig. 3. Considering the rather

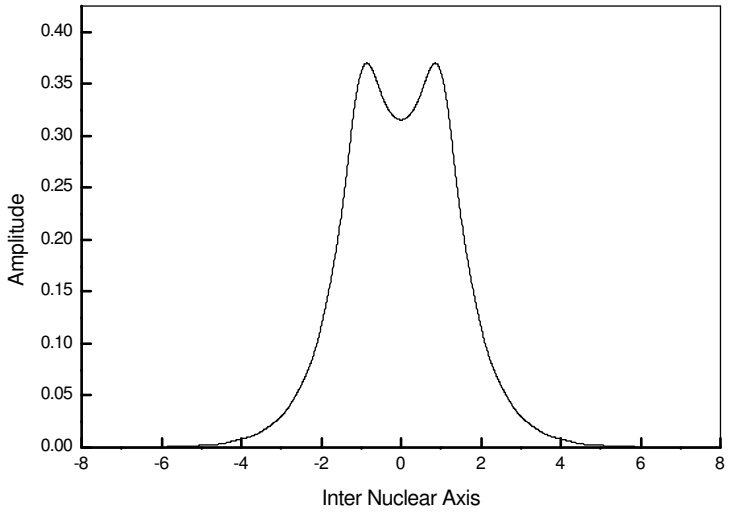

(a)

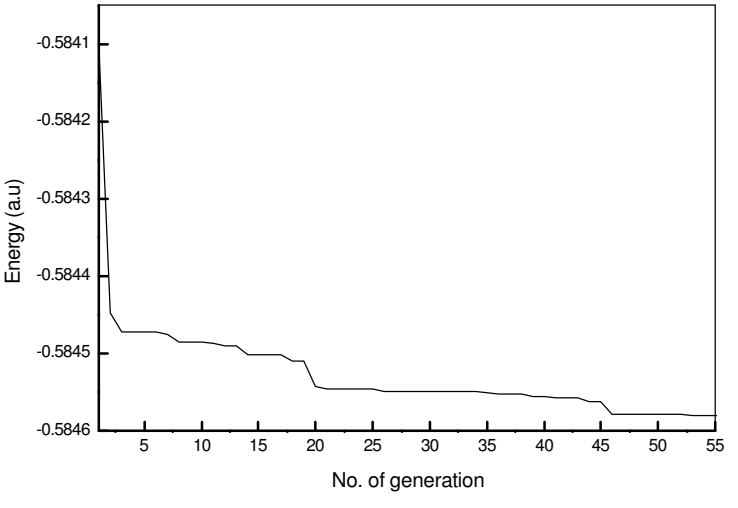

(b)

Fig. 1. (a) The optimized ground state probability amplitude of H_2^+ at internuclear distance $R = 2.0$ a.u. is plotted as a function of the internuclear axis (z) for the calculations of Set I under Type I GA-based search. (b) Evolution of energy for the ground state of the H_2^+ at internuclear distance $R = 2.0$ a.u. in the GA run for the calculations of Set I under Type I GA-based search. The energy refers to the string of the highest fitness in the population.

limited number of grid points the performance of the GA based strategy appears to be encouraging.

Set II: In the calculations of Set II, we have enlarged the uniformly discretized coordinate grid to a collection of $128 \times 128 \times 128$ points. Figure 4 displays the energy-internuclear distance profile fitted to a Morse curve computed by GA. The

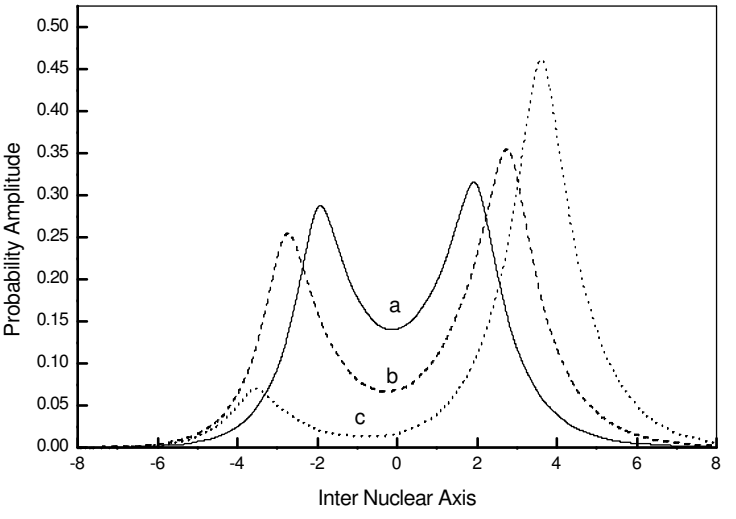

Fig. 2. For the calculations of Set I under Type I GA-based search the optimized amplitude distribution for the ground state of H_2^+ computed at internuclear distance (a) $R = 4.0$ a.u., (b) $R = 5.6$ a.u., (c) $R = 7.2$ a.u. plotted as a function of the internuclear axis (z).

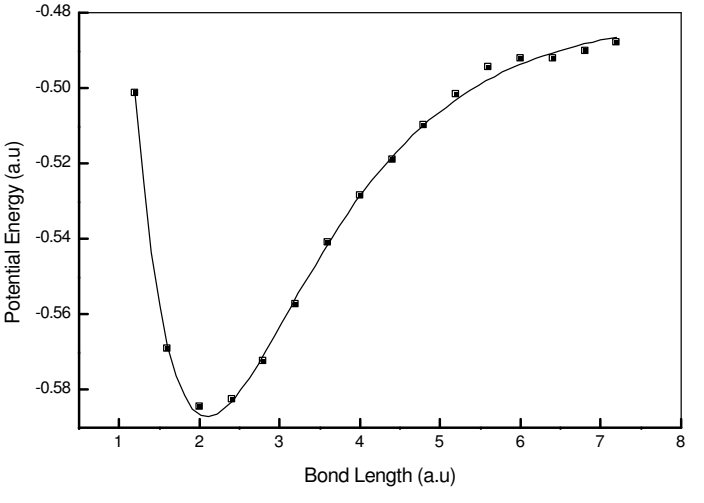

Fig. 3. For the calculations of Set I under Type I GA-based search energy-internuclear distance profile (computed by GA for the ground state of H_2^+ at different internuclear distances) is fitted to a Morse curve.

computed equilibrium internuclear separation (R_e), the dissociation energy (D_e) and total energy at equilibrium separation (V_e) are reported in Table 2. All the computed quantities show marked improvement compared to what was obtained in the previous set of calculations with a smaller number of grid points. The computed probability densities at $R = 4.0$, 5.6 and 7.2 a.u. are displayed in Figs. 5(a)–5(c). It

Table 1. The values of R_e and D_e for the ground state of H_2^+ estimated from the PEC obtained from the two sets of calculations (64 grid points (Set I) and 128 grid points (Set II) using the GA-based Type I method.

Type I results	R_e (a.u.)	D_e (a.u.)
Set I	2.09832	0.10611
Set II	2.03154	0.10738
Experimental[a]	2.00	0.103

[a]Herzberg, Ref. 20, Richardson, Ref. 21.

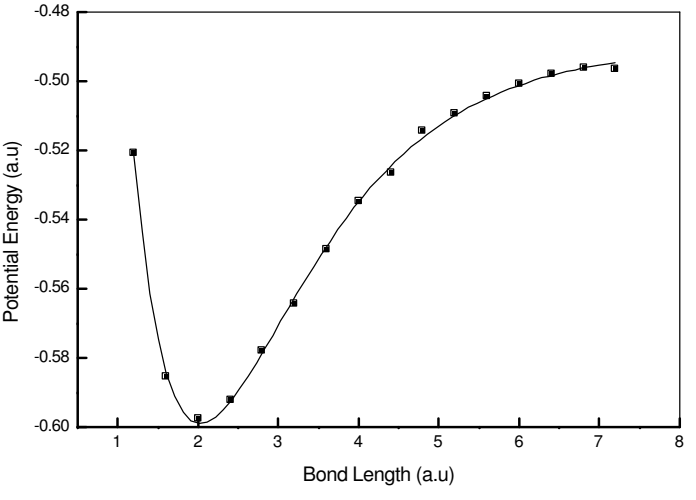

Fig. 4. For the calculations of Set II under Type I GA-based search energy-internuclear distance profile (computed by GA for the ground state of H_2^+ at different internuclear distances) is fitted to a Morse curve.

is clearly seen that at 7.2 a.u. H_2^+ has already dissociated into H + H^+ (Fig. 5(c)). Compared to the 64 point calculation the present calculations reproduce the dissociation behavior much better.

As explained earlier, it is possible to include the internuclear separation R as an additional parameter in strings representing probability amplitude distributions. In that case, internuclear separation evolves genetically along with the amplitude distribution. A single GA run can therefore search out simultaneously the equilibrium internuclear separation, the amplitude distribution corresponding to the equilibrium value of (R_e) and the energy (V_e) at equilibrium.

Table 2. The values of R_e, V_e for the ground state of H_2^+ obtained from the two sets of calculations (Set I and Set II) carried out by Type I and Type II GA-based method compared with previous theoretical results (PTR).

Type of computation	R_e (a.u.)		V_e (a.u.)	
PTR[b]	1.998		−0.602	
	Set I	Set II	Set I	Set II
Type I	2.098	2.031	−0.587	−0.599
Type II	2.169	2.11	−0.586	−0.598

[b]Beckel, Hansen and Peek, Ref. 9.

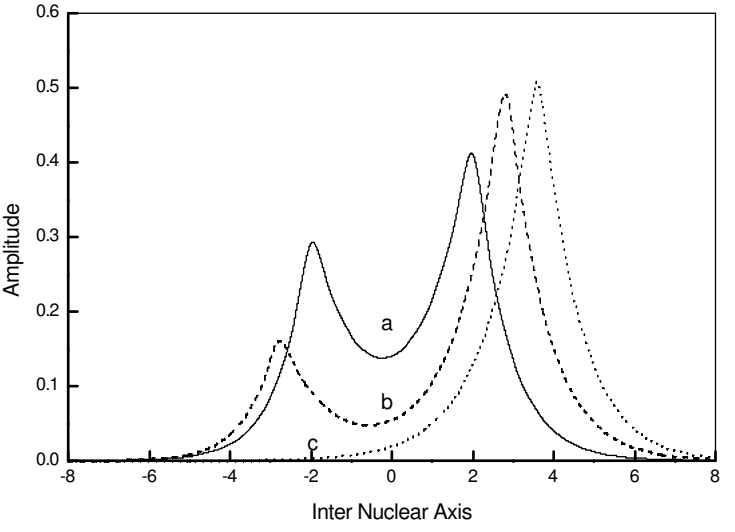

Fig. 5. For the calculations of Set II under Type I GA-based search the optimized amplitude distribution for the ground state of H_2^+ computed at internuclear distance (a) $R = 4.0$ a.u., (b) $R = 5.6$ a.u., (c) $R = 7.2$ a.u. plotted as a function of the internuclear axis (z).

3.2. *Results of Type II calculations*

In calculations under Type II, we have reported results of coupled or simultaneous search for equilibrium amplitude distribution in the ground state (ϕ_e), equilibrium internuclear separation (R_e) and the energy (V_e). The evolution of energy of the best string during such a search is displayed in Figs. 6(a) and 6(b) for the $64 \times 64 \times 64$ (Set I) and $128 \times 128 \times 128$ (Set II) grid point calculations, respectively. Figures 7(a) and 7(b) on the other hand, reveal how the search locates the final equilibrium bond lengths in the two cases. In the 64 grid point calculation (Fig. 7(a)) the initial value of R_e (corresponding to the best string in the initial population) is low ($R_e < 2.10$ a.u.) and shows a steep jump as few generations

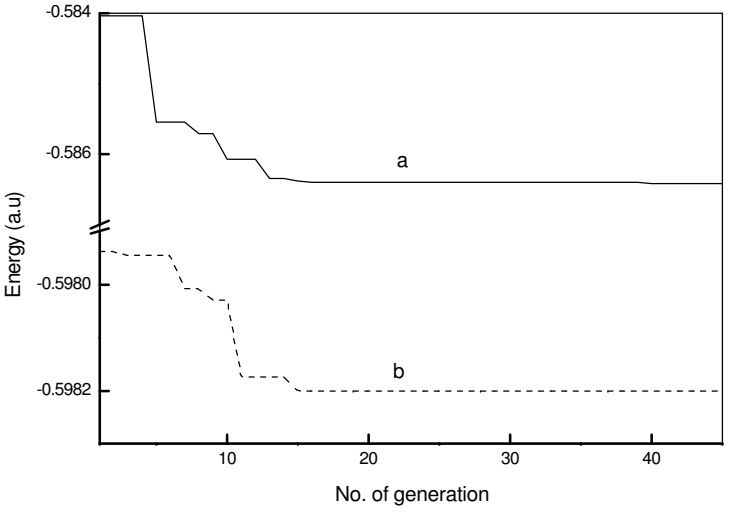

Fig. 6. Under Type II GA-based search (simultaneous search for ϕ_e, R_e, V_e being carried out by GA) evolution of energy of the best string in the GA run is displayed for (a) Set I, and (b) Set II calculations.

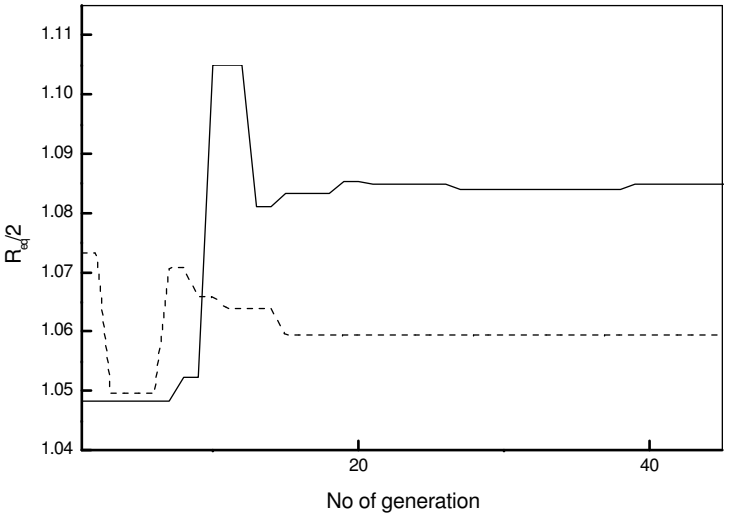

Fig. 7. Under Type II GA-based search (simultaneous search for ϕ_e, R_e, V_e being carried out by GA) profile of the equilibrium bond length of the best string in the GA run is displayed for (a) Set I, and (b) Set II calculations.

elapse. After initial oscillations which are damped quickly, it converges to a value of $R_e = 2.119$ a.u. which is significantly greater than R_e computed from the potential energy curve ($R_e = 2.098$ a.u.) in the Type I calculations. The 128 grid point calculation reveals the same trend, that is, the converged equilibrium internuclear separation R_e (= 2.112 a.u.) being significantly larger than the corresponding R_e

value estimated from the potential energy curve (2.031 a.u.). The origin of the observed differences in R_e obtained from Type I and Type II calculations is not very clear and needs further exploration and analysis. It is evident that in the case of computations with 128 grid points, there has been significant improvements in the quality of results of fully adiabatic calculations compared to what was achieved in the 64 grid point calculations. Since multi-dimensional quadratures become costly with increase in the number of grid points, it is necessary to parallelize the method. Since GA's are trivially parallelizable, it would be worth exploring. We also note that for problems of higher dimensions, it could be profitable to use Monte Carlo method based quadratures, because of their favorable scaling behaviour with respect to dimensionality. If the present method is to be extended beyond one or two electron atoms or molecules, there are several problems that are required to be tackled. The most important is the requirement to ensure the anti-symmetric nature of the wave function strings that are allowed to evolve on the fitness landscape. There are several avenues that could be explored. For example, we may choose strings from family of antisymmetric trial functions and allow the parameters to evolve just as is done in variational Monte Carlo;[22] or, else we may build up the initial population by using strings with fixed nodal structure obtained from the Hartree–Fock determinant. The approach has been tried with diffusion or Greens function Monte Carlo.[10] The GA may be used to optimize the nodal positions also. If the calculations are to be done ignoring electron correlation, the orbitals to be used in DFT or HF type of approach need to be orthonormal — a feature that could be easily introduced in the GA-based objective function by adding a constraint term and resorting to multi-objective optimization of the fitness function. Since for the ground state, it is necessary that the Aufbau principle be followed, a node counting procedure may be introduced to ensure that the total number of nodes is minimized. These possibilities are being explored at present.

4. Conclusions

GAs can be used to solve molecular Schrödinger equation, either for set of fixed nuclear positions or by allowing the nuclear coordinates to float along with the amplitudes of the electronic wave function. For a small number of uniformly distributed grid points 64 or 128, the two type of calculations produce slightly different values equilibrium parameters in test runs on H_2^+. For higher dimensional problems energy calculations by Monte Carlo integration would be necessary to reduce computational cost. The possibilities of using nonuniform grid and multi-dimensional interpolation techniques also need exploration although implementation of the Type II approach with a nonuniform grid would pose nontrivial problems.

Acknowledgments

The authors thank the DST, Government of India for a generous research grant for setting up a Linux PC-cluster, without which the work would not have been

possible. We also thank Prof. S. Ray, head of the computer center for advice and help in setting up the Linux cluster.

References

1. D. R. Bates, K. Ledsham and A. L. Stewart, *Phil. Trans. Roy. Soc. A* **246**, 215 (1953).
2. Burrau, *Det. Kgl Danske Vid Selskal* **7**, 1 (1927).
3. V. Guillemin, Jr. and C. Zener, *Proc. Natl. Acad. Sci.* **15**, 314 (1929).
4. E. A. Hylleraas, *Z. Phys.* **71**, 739 (1931).
5. G. Jaffe, *Z. Phys.* **87**, 535 (1934).
6. R. W. Steven, J. W. Wilkins and M. P. Teter, *Phys. Rev.* **39**, 5819 (1989).
7. H. Wind, *J. Chem. Phys.* **43**, 2956 (1965).
8. W. Kolos, *Acta. Phys. Acad. Sci. Hung.* **27**, 241 (1969).
9. C. L. Beckel, B. D. Hansen and J. M. Peek, *J. Chem. Phys.* **53**, 3681 (1970).
10. I. Kosztin, B. Faber and K. Schulten, *Am. J. Phys.* **64**, 633 (1996).
11. D. E. Makarov and H. Metiu, *J. Chem. Phys.* **108**, 590 (1998).
12. P. Chaudhury and S. P. Bhattacharyya, *Chem. Phys. Lett.* **296**, 51 (1998).
13. R. Saha, P. Chaudhury and S. P. Bhattacharyya, *Phys. Lett. A* **291**, 397 (2001).
14. D. E. Makarov and H. Metiu, *J. Phys. Chem. A* **104**, 8540 (2000).
15. Y. Zeiri, E. Fattal and R. Kosloff, *J. Chem. Phys.* **102**, 1859 (1995).
16. H. Nakanishi and M. Sugawara, *Chem. Phys. Lett.* **327**, 429 (2000).
17. H. Safak, M. Sahin, B. Gülveren and M. Tomak, *Int. J. Mod. Phys. C* **14**, 775 (2003).
18. R. Saha and S. P. Bhattacharyya, *J. Theor. Comput. Chem.* **3**, 325 (2004).
19. J. W. Cooley and J. W. Tukey, *Math. Comput.* **19**, 297 (1965).
20. G. Herzberg, *Spectra of Diatomic Molecules* (Van Nostrand, Princeton, NJ, 1950) [*op. cit.*, p. 534].
21. O. W. Richardson, *Proc. R. Soc. Lond.* **152**, 503 (1935).
22. D. Ceperley, G. V. Chester and M. H. Kalos, *Phys. Rev. B.* **16**, 3081 (1977).